

Towards Using Matrix-Free Tensor Decompositions to Systematically Improve Approximate Tensor-Networks.

Karl Pierce*

*Center for Computational Quantum Physics,
Flatiron Institute, 162 5th Ave., New York, 10010 NY, USA*

E-mail: kpierce@flatironinstitute.org

Abstract

We investigate a novel means to eliminate the propagation of error in approximated tensor-networks via the exact, matrix-free decomposition of full tensor-networks. To demonstrate the effectiveness of the approach, we replace the exact contraction of the particle particle ladder (PPL) tensor diagram in the popular coupled-cluster with single and double excitation (CCSD) method with a low-rank tensor decomposition, namely the canonical polyadic decomposition (CPD). In this way, we replace an $\mathcal{O}(N^6)$ tensor contractions with a reduced-scaling $\mathcal{O}(N^5)$ optimization problem. Additionally, we utilize the iterative structure of CCSD to efficiently initialize the CPD optimization, minimizing the cost of the CPD optimization. We show that accurate chemically-relevant energy values can be computed with an error less than 1 kcal/mol using with a CP rank significantly smaller than the effective rank of the popular the tensor hyper-contraction approach. Importantly, this novel method does not rely on cancellation

of errors, is not dependent on a specific tensor-network, index (physical) ordering of tensors or the choice of tensor decomposition.

1 Introduction

Multi-index arrays, also known as tensors, are an integral tools in the translation of mathematical models into computer algorithms. Unfortunately, tensors are plagued by the so-called *curse of dimensionality* which dictates that the computational effort required to accessing and manipulating data in a tensor grows exponentially with the dimensionality of the tensor. In general, physics-based modeling algorithms, such as those found in electronic structure methods, are comprised of sets of tensor-tensor interactions commonly known as *tensor-networks*. In an effort to overcome the curse of dimensionality associated with evaluating these tensor-networks, researchers often find compressed or low-rank representations of tensor components in these networks. In electronic structure methods there exists an incredibly large and diverse number of studied low rank tensor approximations such as the density fitting approximation¹⁻⁵, orbital localization techniques like pair-natural orbital approach,⁶⁻⁹ and fragmentation schemes¹⁰⁻¹² to name a few. In principle, these techniques are integrated into electronic structure methods by first identifying high-cost tensors-networks and subsequently replacing single or multiple components of these network with a low-rank approximations. However, with each tensor approximation introduced into a tensor-network, a degree of error is also added to the network leading to an undesired propagation of error in the tensor-network. In general, the total accumulated error in an approximated tensor-network grows proportionally with variables such as total length of the tensor-network, total number of approximated tensor and error per approximated-tensor, etc. To mitigate this error propagation, researchers have found some success in using a Taylor series expansion to exactly remove leading order-error in an approximated tensor-networks.^{13,14} However this *robust* approximation approach is not generally applicable to all approximated tensor-networks.

The direction of this work is to extend the application of our previous work^{15,16} to directly approximate any single high-cost tensor-network, not just the two-electron integral tensor. By construction, optimizing a low rank decomposition of a tensor networks provides a direct means to control error. Furthermore, with this approach we replace the cost of contracting a tensor-network with the cost of optimizing the low-rank decomposition. To make our idea more concrete, in this work we construct the particle-particle ladder (PPL) diagram in the coupled cluster with single and double excitations (CCSD) method using a matrix-free canonical polyadic decomposition (CPD). We emphasize, though, that this approach is a general technique that is not limited to this specific tensor-network, the coupled cluster method or the use of the CPD. It should also be noted that the focus of this study is to demonstrate the accurate application of matrix-free optimizations to electronic structure methods and we do not seek to reduce the wall-time of the CCSD method.

The rest of this manuscript is organized as follows. In Section 2 we introduce the coupled cluster method’s particle-particle ladder (PPL) tensor-network, demonstrate how state of the art approximations to this network introduce unintended error and propose a reduced-scaling matrix-free CPD approximation of the PPL tensor-network that provides controllable accuracy. In Section 3 we discuss the details of our computational experiments. In Section 4 we report on the capacity for a matrix-free CPD optimization to replace the exact PPL tensor-network. Finally, Section 5 summarizes our findings and provide future research directions for efficient application of this tensor-network approximation scheme to this and other threads of research.

2 Formalism

2.1 Coupled Cluster and the Particle-Particle Ladder Network

In this work we demonstrate how the decomposition of an entire tensor-networks can more controllably approximate tensor-networks than today’s most standard methods for approxi-

mating tensor-networks, such as the tensor hyper-contraction and density fitting approaches. In this preliminary study, we apply this technique to a representative tensor-network from the popular coupled cluster method. In this section we introduce a high-cost tensor-network from the coupled cluster with single and double excitations (CCSD) method¹ and demonstrate how the state-of-the-art tensor hyper-contraction approximation suffers from propagation of error. In Section 2.3, we propose a method to approximate the tensor-network with a reduced-scaling and controllable accuracy using a matrix-free tensor decomposition optimization strategy.

The goal of the coupled cluster method is to recover ‘dynamical correlation’ which is missing from the Slater determinant picture of Hartree-Fock Theory.¹⁷⁻²⁴ The CCSD method achieves this goal by optimizing the weights of the singly and doubly excited wavefunctions using a coupled set of nonlinear equations, i.e.

$$\begin{aligned}
 0 &= \langle \Phi_i^a | \bar{H} | \Phi_0 \rangle \\
 0 &= \langle \Phi_{ij}^{ab} | \bar{H} | \Phi_0 \rangle
 \end{aligned}
 \tag{1}$$

where \bar{H} is the similarity transformed Hamiltonian, which will not be discussed here. In Eq. (1), the labels i, j, k, \dots are representative of the set of O occupied orbital basis functions and the labels a, b, c, \dots are representative of the set of V unoccupied orbital basis function. The term Φ_i^a represents a singly excited Slater determinant obtained from swapping of the i th occupied orbital function in the Slater determinant ground state, Φ_0 , with the a th unoccupied orbital function and double excited wavefunction, Φ_{ij}^{ab} , is determined in a similar manner. The optimized CCSD weights for Φ_i^a and Φ_{ij}^{ab} are stored in the order-2 t_i^a and order-4 t_{ij}^{ab} tensors, respectively. These weights can then be optimized using standard nonlinear gradient descent optimization techniques. Though the Coupled Cluster family of methods find great success in recovering dynamical correlation, the family is plagued by a restrictively large

¹Please note, a in-depth description of the CC optimization will not be discussed in this work and readers can find extensive reviews on the topic, such as Ref. 17

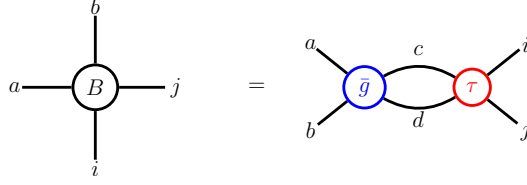


Figure 1: Diagrammatic representation of the particle-particle ladder tensor-network.

computational complexity.

The complexity of CCSD comes from the evaluations of tensor-networks in the residual equations of the nonlinear optimization. The most expensive term in the CCSD residual equations is the particle-particle ladder (PPL) tensor-network

$$B_{ij}^{ab} = \sum_{cd} (g_{cd}^{ab} - 2 \sum_k g_{ck}^{ab} t_d^k) \tau_{ij}^{cd} \quad (2)$$

where $\tau_{ij}^{cd} = t_{ij}^{cd} + t_i^c t_j^d$ and g is the two-electron integral (TEI) tensor that will be discussed in the Section 2.1.1. As an aside, Eq. (2) can be simplified by constructing the intermediate \bar{g} where

$$\bar{g}_{cd}^{ab} = g_{cd}^{ab} - 2 \sum_k g_{ck}^{ab} t_d^k \quad (3)$$

resulting in simplified expression

$$B_{ij}^{ab} = \sum_{cd} \bar{g}_{cd}^{ab} \tau_{ij}^{cd}. \quad (4)$$

Figure 1 shows the diagrammatic expression of the PPL tensor network (Eq. (4)). In this figure, tensors are represented as nodes on a graph and tensor indices are edges. A tensor contraction (or summation over an index) is denoted as a solid line connecting two nodes and, later, a hyperedge (an index which connects more than two nodes) will be denoted as a dashed line. Also, the *order* of a tensor is defined as the number of indices or edges which belong to a tensor. From either of these representations, one can see that the computational

complexity of computing this tensor network is $O^2V^4 \approx \mathcal{O}(N^6)$ where N is a measure of the system-size.

In an effort to reduce the complexity of PPL tensor-network, and therefore the cost of CCSD, theorists have tried approximating components of the PPL tensor-network using various decomposition schemes such as the density fitting approximation and the tensor hyper-contraction. In the following, we will introduce both of these approximations and demonstrate how they can introduce an undesired degree of error propagation in the evaluation of the PPL tensor-network.

2.1.1 The Density Fitting approximation

The most standard approximation made in electronic structure methods is the density fitting (DF) approximation¹⁻⁴ of the two-electron integral (TEI) tensor, g . The elements of the TEI tensor evaluated in a generic set of basis functions $\{\phi\}$ are

$$g_{st}^{pq} = \iint \phi_p^*(r_1)\phi_q^*(r_2)g(r_1, r_2)\phi_s(r_1)\phi_t(r_2)dr_1dr_2. \quad (5)$$

In general $g(r_1, r_2)$ may be any positive kernel and for this work we utilize the Coulomb interaction kernel, i.e. $g(r_1, r_2) \equiv |r_1 - r_2|^{-1}$. The DF approximation is a low-rank representation of the TEI tensor defined as

$$g_{st}^{pq} \stackrel{\text{DF}}{\approx} \sum_X D_s^{pX} D_t^{qX} \quad (6)$$

where the index X here represents an optimized, predetermined auxiliary set of functions which grows linearly with system size² and D is denoted as the DF approximated TEI tensors. One can make Eq. (6) exact by introducing a DF error correction term $(\Delta g)_{qt}^{ps}$ into

²Please note, the DF approximation can also be constructed analytically using a rank-revealing Cholesky decomposition.²⁵⁻²⁸

the equation, i.e.

$$g_{st}^{pq} = \sum_X D_s^{pX} D_t^{qX} + (\Delta g)_{st}^{pq}. \quad (7)$$

Because of the significant compression gained from the DF approximation, the error associated with replacing the TEI tensor with its DF approximation is widely accepted and this work is no exception.²⁹⁻³¹ By this we assume $(\Delta g)_{st}^{pq} \approx 0$ for all DF approximated TEI tensors and in CCSD we will replace all such tensors with their DF approximations, accordingly.

The goal of introducing the DF approximation is to reduce the computational complexity of the tensor-networks in the CCSD method but, unfortunately, the DF approximation fails to reduce the complexity of **all** tensor-networks in the CCSD method. Specifically, it is unable to reduce the complexity of the PPL tensor-network. By substituting the appropriate DF approximated TEI tensors into Eq. (2) we find the following expression

$$B_{ij}^{ab} = \sum_{cd} \sum_X (D_c^{aX} D_d^{bX} - 2 \sum_k D_c^{aX} D_k^{bX} t_d^k) \tau_{ij}^{cd}. \quad (8)$$

To simplify this expression, it is possible to form an intermediate \bar{D} term which is similar to \bar{g} from Eq. (3),

$$\bar{D}_d^{bX} = (D_d^{bX} - 2 \sum_k D_k^{bX} t_d^k). \quad (9)$$

Substituting \bar{D} into Eq. (8) simplifies the expression to be

$$B_{ij}^{ab} = \sum_{cd} \left(\sum_X D_c^{aX} \bar{D}_d^{bX} \right) \tau_{ij}^{cd}. \quad (10)$$

We express the diagrammatic representation of this network in Figure 2 and this figure allows one to easily see that the indices c and d occupy different order-3 D tensors. By construction, the DF approximation maps pairs of orbital indices of a single electronic particle to the same

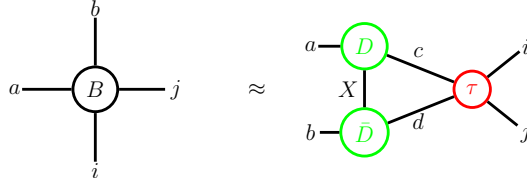


Figure 2: Diagrammatic representation of the DF approximated PPL tensor-network

D tensor and, therefore, this observation means that c and d are indices of different particles. The DF approximated PPL tensor-network does not have a reduced complexity over the canonical PPL tensor-network.

Because the computation of the PPL tensor-network is a significant bottleneck in the CCSD optimization procedure, theorists have studied additional approximations that can effectively reduce the scaling of this tensor-network. These methods include the pseudospectral^{32–41} and the tensor hyper-contraction^{42–58} methods. Although these methods find success in reducing the complexity of the PPL tensor-network, unintentionally, they both introduce an undesired degree of error into the approximation of the PPL tensor-network. In the following section, we will discuss how the popular tensor hyper-contraction is formulated and how its introduction generate error in the PPL tensor-network.

2.1.2 Propagation of error in the THC approximation

As shown in the previous section, the DF approximation cannot reduce the computational scaling of the expensive PPL tensor-network. It is well understood that the tensor hyper-contraction (THC) method^{45–48} can be deployed to reduce the complexity of this tensor-network. Therefore, in this section we introduce the THC approximation and highlight the error it contributes to the construction of the PPL tensor-network. Please note, we choose this example because it’s behavior has been studied and documented^{14,15} and not because this is an issue unique to the THC approximation.

Formally, the THC is a low rank representation where order-4 TEI tensor is represented

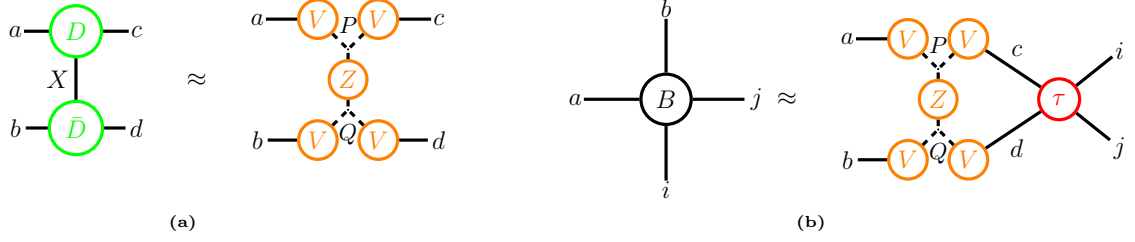


Figure 3: a) Diagrammatic representation of the tensor hyper-contraction approximation b) Diagrammatic representation of the THC approximation of the PPL tensor-network

using five order-2 tensors

$$g_{cd}^{ab} \approx \sum_{PQ} V_P^a V_c^P Z_Q^P V_Q^b V_d^Q \quad (11)$$

The THC representation of the DF approximated TEI can be visualized using Figure 3a. In principle, the THC can be formed by replacing both order-3 DF approximated TEI tensors, D , with the low rank approximation,

$$D_q^{pX} \approx \sum_P V_P^p V_q^P V_X^P \quad (12)$$

where the THC rank index P can be determined analytically using a rank revealing CPD or using a predefined grid basis set and the V tensors are denoted as THC factor matrices. In this construction the THC core matrix is defined as $Z_Q^P = \sum_X V_X^P V_Q^X$. However, Z can also be computed using a low-cost least-squares optimization, which will not be discussed in this work.

We can make the approximation in Eq. (12) exact by introducing a THC approximation error term ΔD :

$$D_q^{pX} = \sum_P V_P^p V_q^P V_X^P + (\Delta D)_q^{pX}. \quad (13)$$

And for simplicity in the following analysis we will define

$$\tilde{D}_q^{pX} = \sum_P V_P^p V_q^P V_X^P \quad (14)$$

where a tilde indicates the THC approximation of a given tensor; therefore

$$D_q^{pX} = \tilde{D}_q^{pX} + (\Delta D)_q^{pX}. \quad (15)$$

If we substitute Eq. (15) into the definition of the DF approximation of the TEI tensor, Eq. (6), we find the following

$$g_{cd}^{ab} = \sum_X (\tilde{D} + \Delta D)_c^{aX} (\tilde{D} + \Delta D)_d^{bX}. \quad (16)$$

Eq. (16) can be expanded into

$$g_{cd}^{ab} = \sum_X \tilde{D}_c^{aX} \tilde{D}_d^{bX} + (\Delta D)_c^{aX} \tilde{D}_d^{bX} + \tilde{D}_c^{aX} (\Delta D)_d^{bX} + (\Delta D)_c^{aX} (\Delta D)_d^{bX} \quad (17)$$

and, as one can see from this expression, the accuracy of the THC approximated TEI tensor depends on the error associated with the THC approximation propagated through Eq. (6). Therefore, similar to Eq. (16), we can define the error in the THC approximation of g as

$$(\Delta g)_{cd}^{ab} = \sum_X (\Delta D)_c^{aX} \tilde{D}_d^{bX} + \sum_X \tilde{D}_c^{aX} (\Delta D)_d^{bX} + \sum_X (\Delta D)_c^{aX} (\Delta D)_d^{bX} \quad (18)$$

which simplifies Eq. (17) into the following expression

$$g_{cd}^{ab} = \tilde{g}_{cd}^{ab} + (\Delta g)_{cd}^{ab} \quad (19)$$

such that $\tilde{g}_{cd}^{ab} \equiv \sum_X \tilde{D}_c^{aX} \tilde{D}_d^{bX}$ is the THC approximation of g .

Introducing Eq. (19) into the PPL tensor-network results in the following expression

$$B_{ij}^{ab} = \sum_{cd} (\tilde{g}_{cd}^{ab} + (\Delta g)_{cd}^{ab}) \tau_{ij}^{cd}. \quad (20)$$

The total, accumulated error in the THC approximated PPL tensor-network is therefore

$$\begin{aligned} \Delta B_{ij}^{ab} &= \sum_{cd} (\Delta g)_{cd}^{ab} \tau_{ij}^{cd} \\ &= \sum_{Xcd} (\Delta D)_c^{aX} \tilde{D}_d^{bX} \tau_{ij}^{cd} + \sum_{Xcd} \tilde{D}_c^{aX} (\Delta D)_d^{bX} \tau_{ij}^{cd} + \sum_{Xcd} (\Delta D)_c^{aX} (\Delta D)_d^{bX} \tau_{ij}^{cd} \end{aligned} \quad (21)$$

which demonstrates how the error associated with the THC approximation is amplified by the DF approximated PPL tensor-network. As an aside, the THC approximated PPL tensor-network is represented in Figure 3b and, using this figure, it is easy to see how the THC approximation can be used to reduce the complexity of the PPL tensor-network.

In the remainder of this work, we eliminate this error propagation by making ΔB a directly controllable element of our tensor-network approximation. To accomplish this task, we compute the canonical polyadic decomposition of the entire DF approximated PPL tensor-network. In the following section, we remind the readers on the details of the canonical polyadic decomposition before using it to approximate the PPL tensor-network.

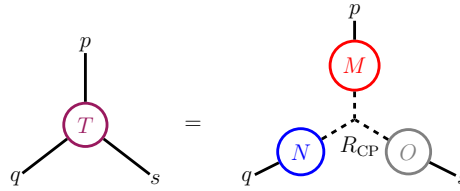


Figure 4: Diagrammatic representation of the canonical polyadic decomposition of a tensor T .

2.2 The Canonical Polyadic Decomposition

The CANDECOMP/PARAFAC, or, simply, the canonical polyadic decomposition (CPD)^{59,60} is a data-sparse representation of higher-order tensors that has been used with various suc-

cess in computational modeling to reduce the cost and/or complexity of the tensor algebra which accompanies physical simulation. The CPD of an order- n tensor can be understood as compression of a single tensor of n modes to a tensor-network of n , order-2 factors all connected by a single hyperedge. For example, given the tensor $T \in \mathbb{R}^{I_P \times I_Q \times I_S}$ the CPD can be expressed as

$$T_{pqs}(\vec{x}) = \sum_r^{R_{\text{CP}}} M_{pr} N_{qr} O_{sr} \quad (22)$$

where $\vec{x} \equiv [M, N, O]$, are the set of CP factor matrices and R_{CP} is the CP rank of the decomposition. The diagrammatic representation of the CPD can be found in Figure 4 where the dashed line represents the CP hyperedge index. As one can see, the topology of the CPD is relatively simple and the effectiveness of the CP compression depends explicitly on the extent of the CP hyperedge (CP rank).^{61,62} Unfortunately, there exist no simple formula which can determine the CP rank. Therefore, the value is revealed by constructing multiple rank- R CPD approximations and choosing the value of R which satisfies the problem's predetermined accuracy thresholds. Therefore, a more accurate representation of the CPD would be

$$T_{pqs}(\vec{x}) = \sum_r^R M_{pr} N_{qr} O_{sr} + (\Delta T)_{pqs} \quad (23)$$

where ΔT is the error in the CPD approximation. Additionally, we will utilize the hat symbol over a tensor to denote a CPD approximation tensor, i.e.

$$\hat{T}_{pqs}(\vec{x}) = \sum_r^R M_{pr} N_{qr} O_{sr}. \quad (24)$$

In electronic structure methods, there exists only a small number of studies which utilize analytically constructed CPD tensors⁶³⁻⁶⁶ and thus the utility of the analytical CPD in the field is still an open question. In these previous studies, Auer et al are able to for-

mally construct low scaling electronic structure methods. However, Auer concedes that, to obtain practical energy values, these CP-based approaches require large CP ranks and are slowed further by the need for periodic re-optimization of CP approximated tensor. In this work, we explore a new application of the analytic CPD to directly approximate high-scaling tensor-network without approximating components of the network. In this way, we replace high-scaling tensor-network contractions with a reduced-scaling optimization with a directly controllable accuracy.³ Furthermore, we extend Auer’s work by preserving the low CP rank of a tensor-network using a fast-update scheme that simultaneously contracts the tensor-network and optimizes a low-rank CPD approximation. In the following sections we demonstrate how we utilize the CPD to approximate the PPL tensor-network in CCSD.

2.3 The CPD approximation of the PPL tensor-network

Our goal is to develop a method to approximate tensor-networks such that the computational complexity of the tensor-network is reduced and the error in the network’s approximation is exactly controllable through the optimization process. In this example, we achieve this goal by representing the DF approximated PPL tensor-network (Eq. (10)) in a low-rank CPD format:

$$B_{ij}^{ab} \approx \sum_r^R \lambda_r \alpha_r^a \beta_r^b \gamma_r^i \rho_r^j, \tag{25}$$

³Please note, in this study we do not preserve the decomposed tensor-network format and choose instead to reconstruct the result of our decomposition.

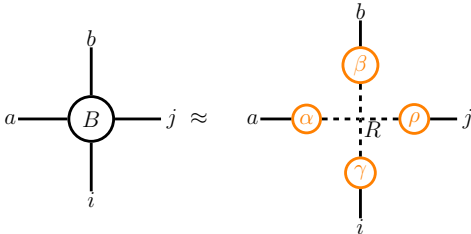


Figure 5: Diagrammatic representation of CPD approximation of the PPL tensor

which we denote the CP-PPL approximation. In this equation R is the rank of the decomposition and α, β, γ and ρ , are the CP factor matrices. The CP factors matrices are column-wise normalized to 1 and the normalization factors are captured in the vector λ_r . As we move forward, we will not explicitly consider λ because, without loss of generality, one can factorize the vector into any one or multiple factor matrices. Additionally, a diagrammatic representation of the CP-PPL approximation is shown in Figure 5.

Similar to the previous approximation, Eq. (25) can be made exact by introducing the CP-PPL error tensor ΔB and, for convenience, defining the CPD approximation $\hat{B}(\vec{x})$ such that

$$\hat{B}_{ij}^{ab}(\vec{x}) = \sum_r^R \lambda_r \alpha_r^a \beta_r^b \gamma_r^i \rho_j^r. \quad (26)$$

Now the exact decomposition can be expressed as

$$B_{ij}^{ab} = \hat{B}_{ij}^{ab}(\vec{x}) + \Delta B_{ij}^{ab}. \quad (27)$$

As one can see, the error in the CP-PPL approximation is directly dependent on the compressibility of the tensor B and the ability to find accurate CP factor matrices for a given rank.

We construct an accurate rank R CP-PPL approximation in a *matrix-free* way by minimizing the following loss function

$$f(\vec{x}) = \min_{\vec{x}} \left(\frac{1}{2} \left\| \sum_{cd} \left(\sum_X D_c^{aX} \bar{D}_d^{bX} \right) \tau_{ij}^{cd} - \hat{B}_{ij}^{ab}(\vec{x}) \right\|_2^2 \right). \quad (28)$$

The error in the approximated CP-PPL tensor-network is exactly the residual $\|B_{ij}^{ab} - \hat{B}_{ij}^{ab}(\vec{x})\|$ which is primarily controlled by the CP rank.⁴ The optimization of \hat{B} is called matrix-free because we effectively 'load' the output of the PPL network into the CPD factor matrices

⁴In principle this fact does not mean that the CPD of the PPL will be a **better** approximation than the THC, just that the error is directly controllable.

without a-priori computing the tensor B . Thus, we attempt to replace the exact PPL tensor-network with the CP-PPL optimization, Eq. (28). It should be noted that in this study \hat{B} is not preserved in the CPD form after a rank R optimization is completed. Instead the tensor is reconstructed into its canonical form for the remainder of the CCSD optimization algorithm. For a given CP rank we minimize Eq. (28) using a simple alternating least squares (ALS) optimization^{67,68} and in the following section we evaluate the computational scaling of each step in the CP-PPL ALS optimization

2.4 Optimizing the CP-PPL tensor-network

In this section, we walk through the computational cost associated with optimizing Eq. (28) using an ALS algorithm. In doing so, we demonstrate that such an optimization has a reduced-scaling compared to the canonical evaluation of the PPL tensor-network. In general, computing a CP-ALS update involves four steps. First, one fixes all but one CPD factor matrix in the cost function, for example the alpha from the n th iteration (α_n). Second, one must take the gradient of the CP loss function, here Eq. (28), with respect to the fixed factor matrix. The gradient of $f(\vec{x})$ with respect to α_n is

$$\begin{aligned} \frac{\partial f(\vec{x}_n)}{\partial \alpha_n} &= \frac{1}{2} \frac{\partial}{\partial \alpha_n} (B^2 - B\hat{B}(\vec{x}_n) - \hat{B}(\vec{x}_n)B + \hat{B}^2(\vec{x}_n)) \\ &= -B \frac{\partial \hat{B}(\vec{x}_n)}{\partial \alpha_n} + \hat{B}(\vec{x}_n) \frac{\partial \hat{B}(\vec{x}_n)}{\partial \alpha_n} \end{aligned} \quad (29)$$

where \vec{x}_n is the set of factor matrices during the n th CPD iteration and

$$\left(\frac{\partial \hat{B}(\vec{x}_n)}{\partial \alpha_n} \right)_{ij}^{rb} = (\beta_n)_r^b (\gamma_n)_i^r (\rho_n)_j^r. \quad (30)$$

Next, one sets the gradient expression from the previous step equal to zero and solves the developed linear problem to determine a new optimal factor matrix, α_{n+1} . This process can be repeated for each of the problem's other factor matrices and can updates are repeated as

many times as necessary. Typically, after a round of updating each factor matrix a stopping condition is assessed. We will discuss appropriate stopping conditions in Section 2.4.1. Next, we will evaluate the cost of computing the CP-PPL gradient and finding an updated CP factor matrix.

As an example of the computational cost of the optimization, we walk through the cost to compute the α_{n+1} factor matrix. Please note, in this analysis we will assume that the CP rank grows linearly with system size based on findings compiled in Section 4. The solution to the ALS gradient update from the CP-PPL cost function for α_{n+1} is

$$[\alpha_{n+1}]_{r'}^a = \sum_{cdbijr} \left(\sum_X D_c^{aX} \bar{D}_d^{bX} \right) t_{ij}^{cd} \beta_r^b \gamma_i^r \rho_j^r \left[\left(\sum_b \beta_r^b \beta_{r'}^b \right) \left(\sum_i \gamma_i^r \gamma_i^{r'} \right) \left(\sum_j \rho_j^r \rho_j^{r'} \right) \right]^{-1}. \quad (31)$$

In the literature, it is common to group all of the terms in the square bracket into a term denoted as $W_{r'}^r$.

$$W_{r'}^r = \left(\sum_b \beta_r^b \beta_{r'}^b \right) \left(\sum_i \gamma_i^r \gamma_i^{r'} \right) \left(\sum_j \rho_j^r \rho_j^{r'} \right). \quad (32)$$

Computation of W can be done efficiently with a cost of $3NR^2 + 2R^2 \approx \mathcal{O}(N^3)$ and its inversion can also be done conveniently using a symmetric, square linear solve algorithm such as the Cholesky decomposition. The inversion of W has a cost of $R^3 \approx \mathcal{O}(N^3)$

Substituting W into Eq. (31) simplifies the equation to

$$[\alpha_{n+1}]_{r'}^a = \sum_r \left[\sum_{Xc} D_c^{aX} \left(\sum_d \left(\sum_b \bar{D}_d^{bX} \beta_r^b \right) \left(\sum_{ij} \gamma_i^r \rho_j^r \tau_{ij}^{cd} \right) \right) \right] [W^{-1}]_{r'}^r \quad (33)$$

Next, one can compute the two inner most contractions $\tau_r^{cd} = \sum_{ij} \gamma_i^r \rho_j^r \tau_{ij}^{cd}$ and $\bar{D}_d^{rX} = \sum_b \bar{D}_d^{bX} \beta_r^b$ which have a cost of $N^4R \approx \mathcal{O}(N^5)$ and $N^3R \approx \mathcal{O}(N^4)$, respectively. The intermediates produced from these contractions can be cached to help minimize the cost of

repeated gradient evaluations. After these contractions the following equation remains

$$[\alpha_{n+1}]_{r'}^a = \sum_r [\sum_{Xc} D_c^{aX} (\sum_d \bar{D}_d^{rX} \tau_r^{cd})] [W^{-1}]_{r'}^r. \quad (34)$$

The terms in the left set of square brackets can be efficiently computed for each value of the rank as

$$\sum_{Xc} D_c^{aX} (\sum_d {}^r \bar{D}_d^X {}^r \tau_d^c) \quad (35)$$

where ${}^r \bar{D}_d^X$ and ${}^r \tau_d^c$ are matrices associated with a specific value of r . In Eq. (35), the sum over d can be computed efficiently using a standard level-3 BLAS *gemm* kernel and the sum over the compound index $\{Xc\}$ can be computed using a standard level-2 BLAS *gemv* kernel. The cost of both of these operations is N^3 for each value of r , leading to an overall scaling of $N^3 R \approx \mathcal{O}(N^4)$. It is obvious that contractions in Eqs. (34) and (35) could be distributed over blocks of r to improve computational performance. However, because we have implemented this decomposition in a serial tensor algebra library we do not exploit this feature in this work. Finally one is left with

$$[\alpha_{n+1}]_{r'}^a = \sum_r D_r^a [W^{-1}]_{r'}^r \quad (36)$$

which can be computed with a cost of $NR^2 \approx \mathcal{O}(N^3)$. As one can now see, the computational complexity of an ALS update is $\mathcal{O}(N^5)$, which is a reduction over the canonical complexity of the PPL tensor-network, please refer to Table 1 for a consolidated representation. In Section 4 we will show that a linear-scaling and modest value of R is necessary to compute chemically accurate energy differences.

We do concede that CPD optimization does have a large computational prefactor due in part to its hyperedge structure. In this work, we do our best to minimize the prefactor by caching intermediate tensors, implementing efficient kernels and developing an effective

Table 1: Cost and Scaling of each contraction in the CP-PPL optimization.

| Contraction | cost | scaling |
|--|-----------|---------|
| $\sum_b \beta_r^b \beta_{r'}^b$ | VR^2 | N^3 |
| $\sum_{ij} \gamma_i^r \rho_j^r \tau_{ij}^{cd}$ | O^2V^2R | N^5 |
| $\sum_b D_d^{bX} \beta_r^b$ | V^2XR | N^4 |
| $\sum_d D_d^{rX} \tau_d^{rc}$ | V^2XR | N^4 |
| $\sum_{Xc} D_c^{aX} \tau_{Xc}^r$ | V^2XR | N^4 |
| W^{-1} | R^3 | N^3 |
| $\sum_r D_r^a [W^{-1}]_{r'}^r$ | VR^2 | N^3 |

initialization, discussed in Section 2.4.2. However, ultimately this work is a starting point to a more advanced study and application of matrix-free optimization to electronic structure methods. In future work, we plan to integrate localization and randomized linear algebra techniques to reduce computational prefactors. As this is a preliminary study into the application of matrix-free decompositions to replace tensor-network contractions we focus less on the reduced-scaling impacts of this work and more on the effects our method has on the CCSD residual equation and subsequent optimization accuracy. In this next section we develop a new and reduced-scaling metric to terminate the matrix-free CP-PPL ALS minimization.

2.4.1 Low cost CPD stopping condition

The canonical stopping condition for the CPD is based on the change in the fit of approximation. The fit of the approximated PPL tensor is

$$\Delta_n = 1.0 - \frac{\|B - \hat{B}(\vec{x}_n)\|}{\|B\|} \quad (37)$$

and, therefore, the canonical stopping condition is

$$\Delta_n - \Delta_{n-1} < \epsilon \quad (38)$$

where ϵ is the chosen threshold value. However, for this matrix-free decomposition, computing the fit is prohibitively expensive (with a complexity of $\mathcal{O}(N^6)$). We will breakdown the cost of the canonical stopping condition.

The numerator of Eq. (37), also defined as the residual, and can be expanded as

$$\|B - \hat{B}(\vec{x}_n)\| = \sqrt{B^2 - 2 * B\hat{B}(\vec{x}_n) - \hat{B}^2(\vec{x}_n)}. \quad (39)$$

The second and third terms under the square root can be computed with relatively low-cost; the term $B\hat{B}(\vec{x}_n)$ is partially-formed during the computation of the CPD gradient and, therefore, formally has a complexity of $\mathcal{O}(N^5)$ as demonstrated previously. Additionally, the term $\hat{B}^2(\vec{x}_n)$ can be computed by leveraging the CPD format

$$\hat{B}(\vec{x}_n)\hat{B}(\vec{x}_n) = \sum_{rr'} [((\alpha_n)^T \alpha_n) * ((\beta_n)^T \beta_n) * ((\gamma_n)^T \gamma_n) * ((\rho_n)^T) \rho_n]_{r'}. \quad (40)$$

and has a complexity of $\mathcal{O}(N^3)$. Unfortunately, any attempt to construct B or B^2 using the PPL tensor-network results in a $\mathcal{O}(N^6)$ computational complexity.

In principle, it would be possible to forgo a check completely and simply require a certain number ALS iterations be completed. However, it would be preferred to have some metric to effectively stop the optimization in as few steps as possible. Therefore, in this work we introduce the new metric

$$\eta = \frac{\|\hat{B}(\vec{x}_n) - \hat{B}(\vec{x}_{n-1})\|}{\|\hat{B}(\vec{x}_{n-1})\|} \quad (41)$$

The numerator of η can be expanded as

$$\eta_{\text{num}} = \sqrt{\hat{B}^2(\vec{x}_n) - 2\hat{B}(\vec{x}_n)\hat{B}(\vec{x}_{n-1}) + \hat{B}^2(\vec{x}_{n-1})} \quad (42)$$

and all terms in this residual can be efficiently computed in $\mathcal{O}(N^3)$ time using the same

mechanism found in Eq. (40). The CPD is then terminated when $\eta < \epsilon$ for some chosen ϵ and an appropriate value of ϵ will be discussed in Section 4. As with most optimization problems, the quality and duration of the CPD optimization can strongly depend on the initial guess. Therefore, in the following section we will propose an improved initial guess strategy to minimize the required number of ALS iterations and therefore the cost of computing the CPD.

2.4.2 An improved initial guess strategy

In general, nonlinear optimizations require an unknown (potentially large) number of iterations and the number of iterations can depend strongly on the quality of an initial guess. In this application we require the nonlinear CPD optimization be computed many times during the course of a CCSD non-linear optimization. It is, therefore, in our best interest to find a high-quality initial guess strategy that minimizes the number of CPD optimization iterations.

In our previous work, we have found that a reasonable starting guess is a collection of random numbers chosen from a uniform distribution between $[-1, 1]$. In this work, too, we see that this guess puts the CPD solver in a good position to converge to a relatively accurate optimization in as few as 13 iterations. However consider the following, if we choose a random guess for each CP-PPL optimization, during each CCSD iteration, we are effectively treating each PPL tensor-network as an independent CPD problem. However, we hypothesize that for a single CCSD run the optimized CP-PPL factor matrices during the n th CCSD iteration are close in optimization space to the CP-PPL factor matrices of the $m > n$ CCSD iteration. In this way, we are saying that there is some relationship between optimized CPD approximations of a given tensor-network which are components of a iterative gradient optimization method, such as CCSD. Therefore our proposed strategy is to find and cache a set of optimized CP-PPL factor matrices during the n th CCSD iteration and later use such factors as an initial guess for a later CP-PPL optimization. A more

complete description of our initial guess procedure be presented and analyzed in Section 4. Next, we describe the computational experiments used to validate this work.

3 Computational details

All DF approximated CCSD calculations have been computed using a developmental version of the massively parallel quantum chemistry (MPQC) software package⁶⁹ and computations were run on the Flatiron institute Scientific Computing Core’s (SCC) Rusty cluster using the standard Rome nodes that are equipped with 2 AMD EPYC 7742 processors that each have 64 CPU cores and 512 GB of memory. Each CC calculations was run on a 16 core partition of a single Rome CPU with each partition containing 128 GB of memory. The CP approximation of the order-4 PPL tensor-network were computed using a standard alternating least squares (ALS) method^{67,68} as discussed previously. Using the initialization schemes discussed in Section 2.4.2, we see rapid convergence to high accuracy approximation and the full extent of these optimizations will be discussed in Section 4. All CPD optimizations that utilize the canonical CP stopping condition, Eq. (37), use a convergence criteria of $\epsilon = 10^{-3}$ which was found to be sufficiently accurate in our previous published results.^{14,15} We compare this work to the THC approximation of the PPL tensor-network and the THC approximation was computed using an analytic CP decomposition of the order-3 DF integral tensors, as presented in our previous work.¹⁴ The focus of our study is small water clusters with between 1 to 5 molecules in the TIP4P optimized geometry^{70,71} For the the water cluster we utilized the cc-pVDZ-F12 (DZ-F12) basis set accompanied by the corresponding aug-cc-pVDZ-RI (DZ-RI) DF basis set.^{29,72} In the following section we present our findings from these experiments.

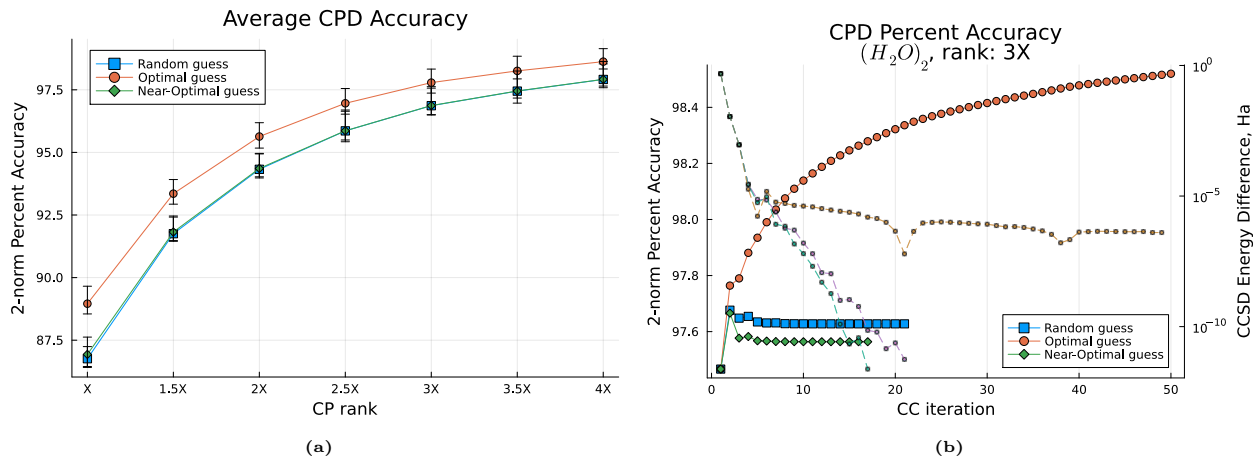


Figure 6: (a) Average CP-PPL percent accuracy at different ranks using three CPD initialization schemes. Error bars represent maximum and minimum percent accuracy across water clusters. (b) For a CCSD optimization of a two-water cluster using a CP rank of $3X$ the CPD 2-norm percent accuracy of the PPL decomposition for each CC iteration (solid lines) and the CCSD energy convergence in Hartree for each iteration (dashed lines)

4 Results

In this section, we demonstrate that it is possible to accurately replace the exact computation of the CCSD PPL tensor-network with a low-rank, matrix-free tensor factorization. Further, we establish an understanding of the following CP-PPL parameters: initial guess strategy, CP rank and CPD stopping condition. And we consider the computational limitations of this approach.

4.1 Role of the Initial Guess

First, we investigate the role of initial guess in our CPD and CCSD optimization. In this work we use three different initial guess strategies:

- with "Random guess" we initialize each CPD with a set of randomly initialized factor matrices;
- with "Optimal guess" we initialized every CPD with the output of the previous CPD optimization; and
- with "Near-Optimal guess" we initialize the current CPD with a previous cached set

of factor matrices from a previous optimization. The cached factor matrices are taken from the $n - 5$ iteration of a previously CPD optimization. If the current CPD optimization does more than 5 iterations, then the factor matrices are cached. Else, the current optimized factor matrices are not cached for later use and a previously cached set is used in the subsequent optimization.

For all of these schemes, the first CPD optimization of a network always uses the "random guess". Additionally for the "Near-Optimal guess" scheme the value 5 was chosen to be arbitrary close enough to the end of the optimization for later optimizations to converge quickly and far enough away to consistently optimize the CP-PPL to nearly the same 2-norm accuracy, as one can see in Figure 6b.

In Figure 6a, we plot the 2-norm based percent accuracy of the CP-PPL where the percent accuracy is computed as 100 times the CP fit, Eq. (37). This figure shows that, as expected, increasing the CP rank directly improves the accuracy of the approximation of B . To compile the data in Figure 6a we first average the CPD accuracy over the number of CCSD iterations for each molecule. Then we average the averaged CPD accuracies over the set of molecules tested. Figure 6a shows that the 'Random' and 'Near-Optimal' guesses produce roughly the same CP-PPL approximation. While the 'Optimal guess' initial guess scheme produces a better CPD optimization on average than the other two initial guess schemes. This result makes more sense when one examines Figure 6b.

In Figure 6b the optimized CP-PPL accuracy (solid lines) and CCSD energy difference in Hartree (dashed lines) are shown for each iteration of a CC optimization of a 2 water-molecule cluster using a CP rank of $3X$. In this work, the CCSD optimization is terminated when the CCSD energy difference is less than the tolerance value of 10^{-10} Ha. One can see that with the 'Optimal guess' scheme, because the CP optimization continues from the previous iterations best answer, the CP-PPL improves consistently throughout the course of the CCSD optimization. However, this accuracy improvement is not exactly desirable as it causes the CC optimization to "swamp" and never reach its target energy convergence

of 10^{-10} Ha. In no single CP-PPL based CCSD optimization computed with the ‘Optimal guess’ scheme does the CCSD loop converge to the the requested energy difference cutoff in 50 iterations. Perhaps this suggests an issue with the robustness of the standard Jacobi-DIIS CCSD solver and that such a solver only preforms well with consistently approximated terms in it’s gradient expression. In future work, we hope to garner a better understanding of the interplay between the CPD optimization/approximation of the PPL ladder diagram and the CC optimization landscape to resolve this swamping issue. Next, we look to compare the rank and accuracy of the CP-PPL to the established tensor hyper-contraction scheme.

4.2 Error Propogation analysis

In this section we hope to gain perspective about the CP-PPL approach by comparing it’s results to that of the standard tensor hyper-contraction method. We use Figure 7 to

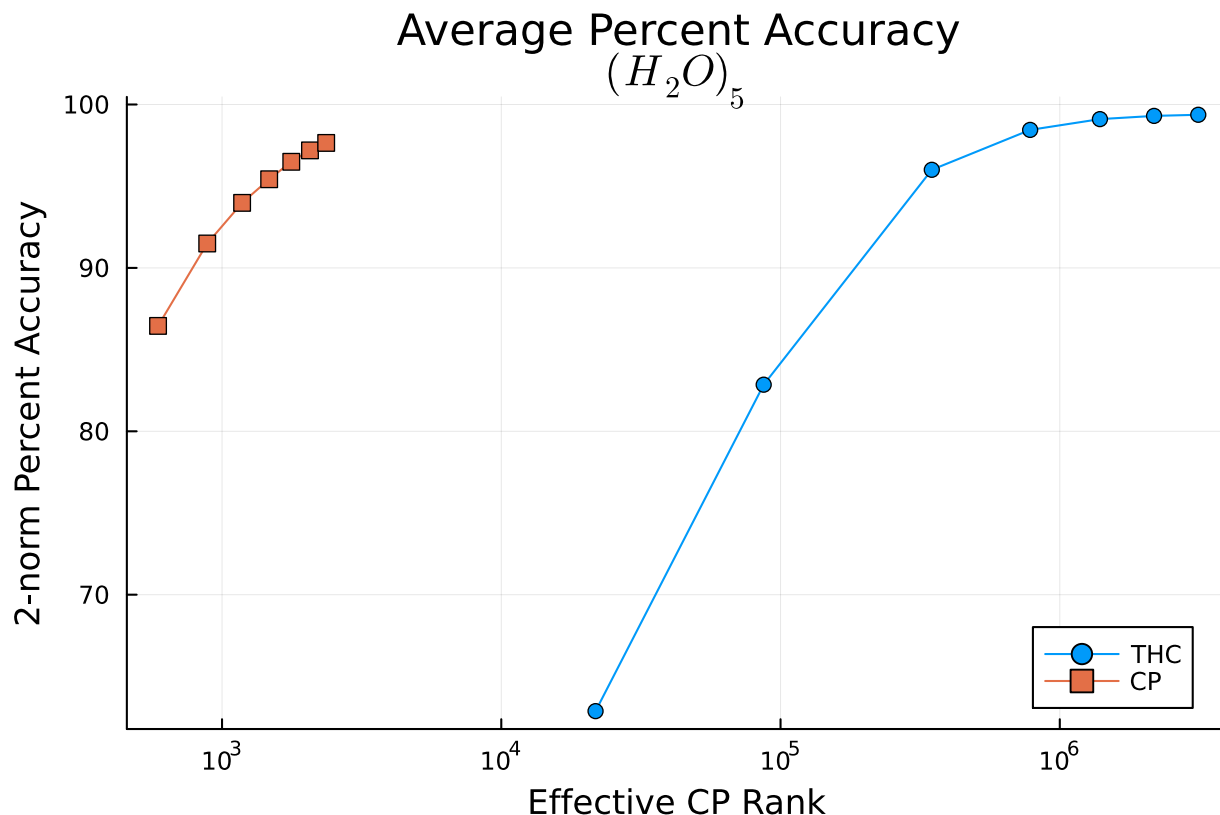


Figure 7: The 2-norm percent accuracy of approximated PPL networks for a 5 water molecule clusters. Effective CP rank of the THC is computed as R_{THC}^2 and the CP-PPL is computed using the "Near-Optimal guess".

compare the accuracy of the CP-PPL approximation to the THC approximation of the PPL tensor-network. Using this figure we can resolve what values for the CP rank result in an equivalently accurate approximations of the PPL tensor-network. This figure shows that the effective CP rank of the THC approximation must be at least one order of magnitude larger than the rank of the CP-PPL approximation. We compute the effective CP rank of the THC approximation by transforming the THC approximation into an order-4 CPD, as we have done in previous studies. The transformation of THC, i.e. Eq. (11), into a CPD can be performed merging the THC rank's P and Q into a compound index $w = \{P, Q\}$. Now we find

$$g_{cd}^{ab} \approx \sum_w \lambda_w V_w^a V_w^b V_c^w V_d^w \quad (43)$$

where

$$V_w^a \equiv V_{\{P,Q\}}^a \equiv V_P^a \otimes \mathbb{I}_Q, \quad (44)$$

$$V_w^b \equiv V_{\{P,Q\}}^b \equiv V_Q^b \otimes \mathbb{I}_P, \quad (45)$$

$$V_c^w \equiv V_c^{\{P,Q\}} \equiv V_c^P \otimes \mathbb{I}_Q, \quad (46)$$

$$V_d^w \equiv V_d^{\{P,Q\}} \equiv V_d^Q \otimes \mathbb{I}_P, \quad (47)$$

$$\lambda_w \equiv Z_Q^P \quad (48)$$

This means that the rank of the effective order-4 decomposition of the TEI tensor using the THC approximation is the square of the THC rank. This over-parameterization is handled efficiently in the THC format, leading to reduced-scaling THC based algorithms. Furthermore, this over-parameterization helps to efficiently reduce the error in the decomposition, which leads to reduced error propagation compared to CP approximation of tensor-network component tensors. However, because our new approach does not suffer from error propagation, we are able to exploit the problems' true rank, leading to significantly lower effective

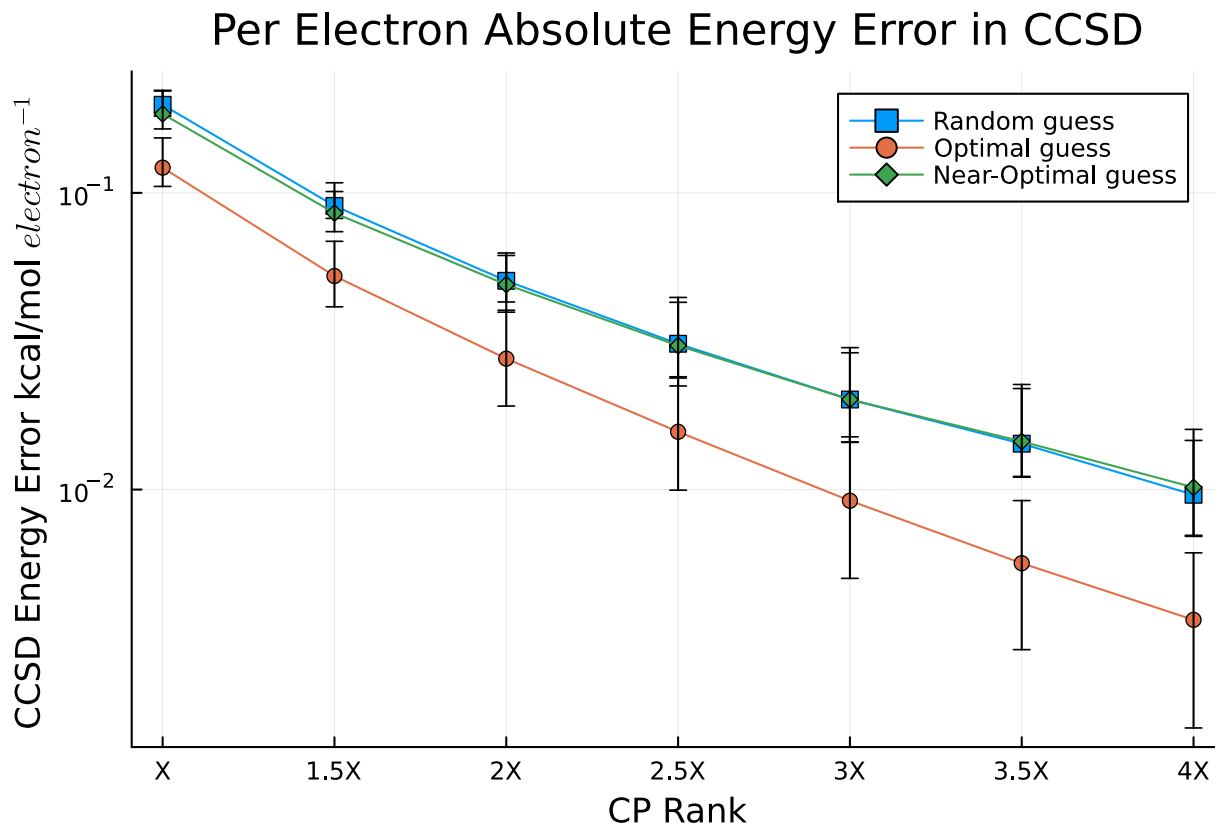


Figure 8: Absolute CCSD energy error per electron for clusters of 1 to 5 water molecules versus CP rank using the various initial guess schemes. Error bars represent maximum and minimum CCSD energy error. The 'Random guess' and 'Near-Optimal guess' schemes were converged to a CCSD energy difference of 10^{-10} Ha however all 'Optimal guess' computations did not converge in 50 CCSD iterations.

CP ranks. This result is consistent to our findings in the matrix-free approximation of the order-4 TEI tensor. Next, we demonstrate that the CP-PPL method is able to reliably produce accurate electronic correlation energies.

4.3 Analyzing the accuracy of the CPD-PPL

Here we show that sufficiently accurate and systematically improvable energies values can be computed using the CP-PPL approach. First, Figure 8 shows the average per electron energy error compared to the canonical DF approximated CCSD energy for the water clusters. As the CP-PPL approximation improves, all initial guess strategies find increasingly accurate energy values. The 'Random guess' and 'Near-Optimal guess' approaches both find nearly identical energy values and interestingly, the 'Optimal guess' scheme find significantly more

accurate CCSD energy values for every molecule and at every rank. However, Figure 9

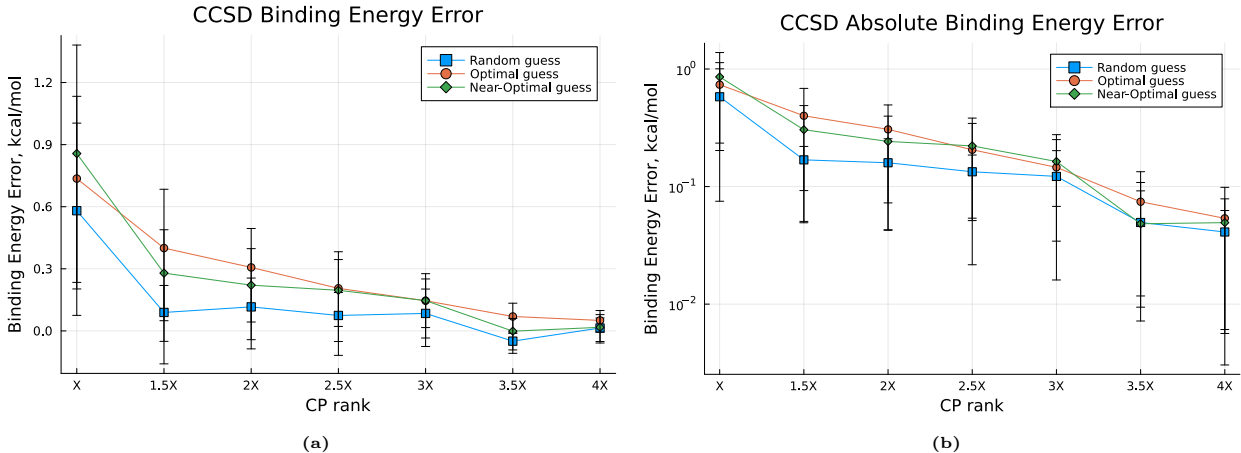


Figure 9: (a) Signed and (b) unsigned binding energy error in kcal/mol versus CP rank for clusters of 2 to 5 water molecules. Error bars represent maximum and minimum binding energy error for a fixed CP rank.

shows that the more accurate CCSD energies found using the ‘Optimal guess’ scheme do not categorically translate to more accurate energy differences. In fact, in this example, the scheme always finds higher error in the binding energy of water when compared to the ‘Random guess’ scheme. Most likely, the lower accuracy binding energies are related to the fact that the ‘Optimal guess’ does not converge the computed CCSD energies below 10^{-6} Ha. While the other approaches may more systematically produce errors that result in fortuitous cancellation of error. Most importantly from Figure 9, one can see that only a modest CP rank of 1.5X is required to compute the binding energy with an accuracy beyond chemical accuracy, 1 kcal/mol. Though, we recommend a slightly greater rank between [3.5X, 4X] to find a relative accuracy of beyond 0.1 kcal/mol. Furthermore, these energy results demonstrate that the rank of the CP-PPL approximation is proportional to the DF fitting basis and therefore grows linearly with system size. In the final section we introduce our reduce scaling convergence CPD criteria and discuss performance of the CP-PPL

4.4 CPD convergence and CP-PPL Performance

Here we introduce our reduce-scaling CPD convergence criteria and show the wall-time performance of the CP-PPL approach. Thus far, our results have used the canonical stopping

condition, i.e. Eq. (37). As discussed previously this stopping condition depends on the norm of the PPL tensor, which has an irreducible $\mathcal{O}(N^6)$ scaling. In Figures 10–12, for the data labeled " N^3 Stopping Condition" we replace the canonical stopping condition with the reduced-scaling stopping condition from Eq. (41). In general, the choice of stopping condition threshold, ϵ , is an arbitrary decision and was chosen to replicate the balance between CP-PPL accuracy and number of least squares iterations found using the canonical stopping condition. Here we do not perform a deep evaluation of the new stopping condition and choose the stopping condition of $\epsilon = 0.02418$ based on a simple heuristic: we choose a value of ϵ such that the water dimer molecule with a CP rank of $2X$ completes its CP-PPL optimization in 16 ALS iterations using the "Random Guess" initialization scheme. Additionally, all calculations which use the reduced-scaling stopping condition also utilize the improved 'Near-Optimal guess' scheme. Figure 10 shows that this initial guess scheme realizes nearly identical results for per-electron energy and absolute binding energy errors when compared to the canonical stopping condition.

Finally, because the CP-PPL is technically a reduced scaling approach, we show the cost of the optimizations in Figures 11 and 12. As discussed earlier, the point of this work is not to realize a wall-time improvement over the canonical contraction of the PPL diagram though, for completeness, we discuss the theoretical cross over. This matrix-free CPD optimization

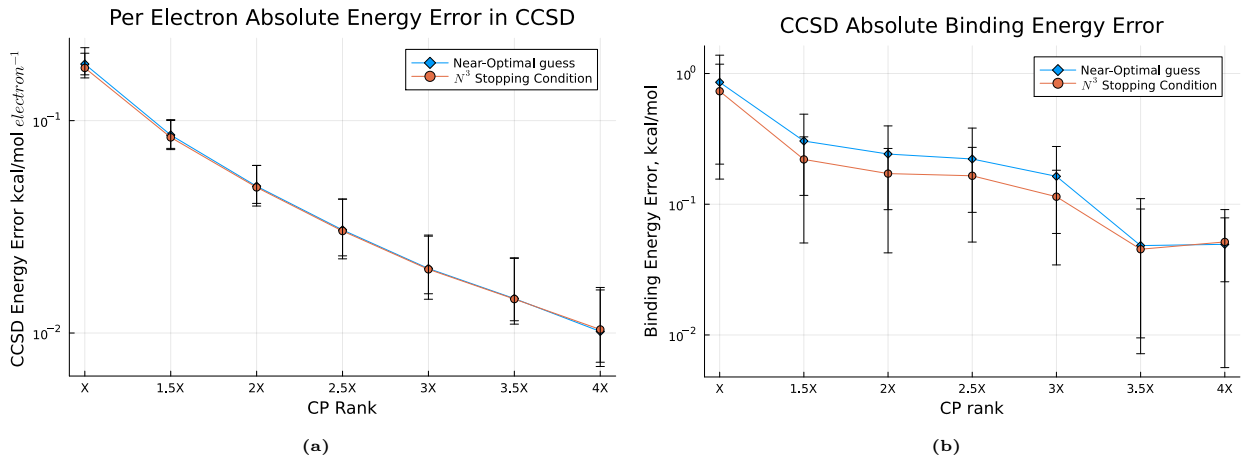


Figure 10: (a) Absolute CCSD energy error per electron for clusters of 1 to 5 water molecules versus CP rank. Error bars represent maximum and minimum CCSD energy error. (b) Absolute binding energy error in kcal/mol versus CP rank for clusters of 2 to 5 water molecules. Error bars represent maximum and minimum binding energy error for a fixed CP rank.

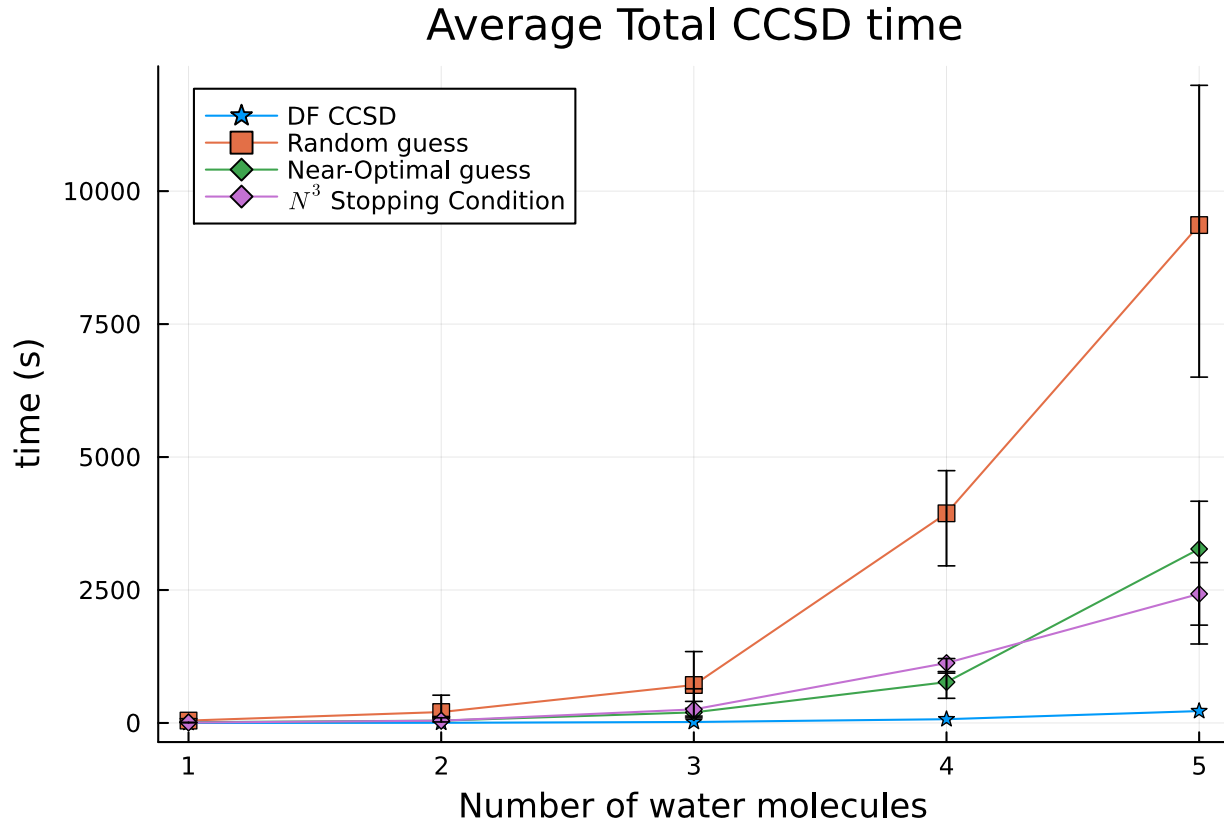


Figure 11: Total time to compute the CCSD energy using the CP-PPL tensor-network optimization averaged across the values of CP rank. Error bars represent the maximum and minimum recorded times

has a leading cost of $(V^2O^2R_{CP-PPL})$ per CPD ALS update, where V is the dimension of the unoccupied orbital space and O is the dimension of the occupied orbital space. For the CPD approach there is an additional $(V^2O^2R_{CP-PPL})$ cost to reconstruct the PPL tensor after the CPD optimization. The canonical PPL has a computational scaling of (V^4O^2) . Theoretically there should be a cross over in cost when $V^2 > R_{CP-PPL}(N_{ALS} + 1)$ where N_{ALS} is the number of ALS iterations. In this work, we have show that a CP rank of $4X$ is sufficiently accurate and an acceptable value of X is on the order of $2V$. Therefore, this approach should find advantage over the canonical PPL when $V > 8(N_{ALS} + 1)$. The ALS iterations for this method depends on the ALS stopping condition and initial guess but is typically between 8 and 30 which would put the theoretical cross over point between $[64, 240]$ unoccupied orbitals. However, because the CPD has a relatively high prefactor, as discussed in Section 2.3 it is difficult to realize this cross-over. In this direction, we seek

to improve the timing of the code by distributing the optimization algorithm and utilizing randomized/interpolation based methods to further reduce the prefactor of the CPD of tensor-networks.

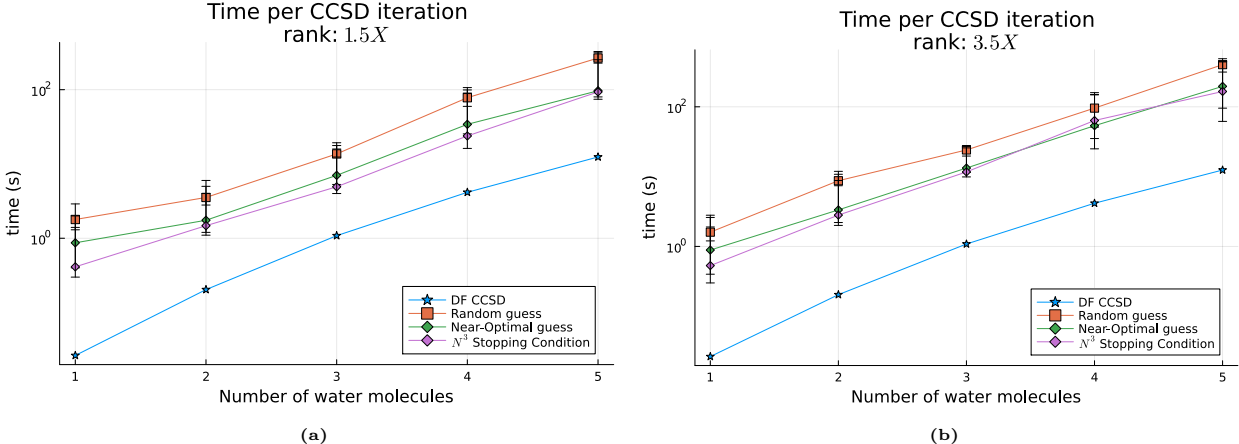


Figure 12: CCSD per iteration cost versus number of water molecules. Results were compiled using a CP rank of (a) $1.5X$ and (b) $3.5X$. Error bars represent maximum and minimum per iteration time.

5 Conclusions

We have shown that it is possible to eliminate error propagation in the approximation of tensor-networks by replacing the network with a low-rank tensor decomposition. This idea is not limited to a specific tensor-network or decomposition topology and here we specifically investigate the approximation of the density-fitting particle particle ladder (PPL) tensor-network in the coupled cluster with single and double excitations (CCSD) method using the canonical polyadic decomposition (CPD). We find that computing a CPD approximation of the PPL tensor-network can be done accurately with a significantly small effective rank (when compared to alternative approximation to this tensor network such as the tensor hyper-contraction approach) that grows linearly with chemical system size. These results complement our previous results from the investigation into the order-4 CPD of the coulomb integral tensor-network.¹⁵ Furthermore, we utilize the iterative nature of CCSD to construct an effective CPD initial guess strategy that minimizes the cost of the CPD optimization.

Unfortunately, we find that the approximation of the PPL ladder with this new scheme can have a significant effect on the optimization of the CCSD wavefunction. To overcome this problem in a standard Jacobi-DIIS CCSD optimization loop, measures must be taken to ensure a consistent CPD approximation. We believe that these results warrant an investigation into CCSD solvers with improved stability.

In future works, we will study methods to improve the optimization of tensor-networks which are computed inside of iterative optimization schemes like coupled cluster. Additionally, we seek to replace more complex and higher-order tensor-networks such as the particle-particle ladder diagram found in the rank-reduced coupled cluster with single, double and triple excitations (CCSDT).⁷³ Finally, we look to use more elaborate strategies to better and more quickly decompose tensor-networks. These strategies include using sparsity constraints, utilizing low-cost nonlinear optimization schemes, and using random/interpolation methods to more quickly approximate the gradient of tensor-networks.

Acknowledgement

This work was supported by the Flatiron Institute and the Simons foundation. We also acknowledge the Scientific Computing Core (SCC) at Flatiron Institute (<https://www.simonsfoundation.org/flatiron/scientific-computing-core/>) for providing computational resources and technical support that have contributed to the results reported within this paper. Furthermore it is important to acknowledge Dr. J Kaye and Dr. A. Dawid for their valuable discussions and the author thanks Mina Mandic for contributing in the early stages of the project.

References

- (1) Whitten, J. L. Coulombic Potential Energy Integrals and Approximations. *J. Chem. Phys.* **1973**, *58*, 4496–4501.

- (2) Dunlap, B. I.; Connolly, J. W. D.; Sabin, J. R. On First-Row Diatomic Molecules and Local Density Models. *J. Chem. Phys.* **1979**, *71*, 4993.
- (3) Vahtras, O.; Almlöf, J.; Feyereisen, M. W. Integral approximations for LCAO-SCF calculations. *Chem. Phys. Lett.* **1993**, *213*, 514–518.
- (4) Jung, Y. Chemical Theory and Computation Special Feature: Auxiliary Basis Expansions for Large-Scale Electronic Structure Calculations. *Proc. Natl. Acad. Sci.* **2005**, *102*, 6692–6697.
- (5) Mintmire, J.; Dunlap, B. Fitting the Coulomb Potential Variationally in Linear-Combination-of-Atomic-Orbitals Density-Functional Calculations. *Phys. Rev. A* **1982**, *25*, 88–95.
- (6) Ahlrichs, R.; Lischka, H.; Staemmler, V.; Kutzelnigg, W. PNO–CI (Pair Natural Orbital Configuration Interaction) and CEPA–PNO (Coupled Electron Pair Approximation with Pair Natural Orbitals) Calculations of Molecular Systems. I. Outline of the Method for Closed-shell States. *J. Chem. Phys.* **1975**, *62*, 1225–1234.
- (7) Ahlrichs, R.; Keil, F.; Lischka, H.; Kutzelnigg, W.; Staemmler, V. PNO–CI (Pair Natural-orbital Configuration Interaction) and CEPA–PNO (Coupled Electron Pair Approximation with Pair Natural Orbitals) Calculations of Molecular Systems. III. The Molecules MgH₂, AlH₃, SiH₄, PH₃ (Planar and Pyramidal), H₂S, HCl, and the Ar Atom. *J. Chem. Phys.* **1975**, *63*, 455–463.
- (8) Neese, F.; Wennmohs, F.; Hansen, A. Efficient and Accurate Local Approximations to Coupled-Electron Pair Approaches: An Attempt to Revive the Pair Natural Orbital Method. *J. Chem. Phys.* **2009**, *130*, 114108.
- (9) Neese, F.; Valeev, E. F. Revisiting the Atomic Natural Orbital Approach for Basis Sets: Robust Systematic Basis Sets for Explicitly Correlated and Conventional Correlated *Ab Initio* Methods? *J. Chem. Theory Comput.* **2011**, *7*, 33–43.

- (10) Kitaura, K.; Ikeo, E.; Asada, T.; Nakano, T.; Uebayasi, M. Fragment Molecular Orbital Method: An Approximate Computational Method for Large Molecules. *Chem. Phys. Lett.* **1999**, *313*, 701–706.
- (11) Kristensen, K.; Ziolkowski, M.; Jansik, B.; Kjaergaard, T.; Jorgensen, P. A locality analysis of the divide–expand–consolidate coupled cluster amplitude equations. *J. Chem. Theory Comput.* **2011**, *7*, 1677–1694.
- (12) Guo, Y.; Becker, U.; Neese, F. Comparison and Combination of “Direct” and Fragment Based Local Correlation Methods: Cluster in Molecules and Domain Based Local Pair Natural Orbital Perturbation and Coupled Cluster Theories. *J. Chem. Phys.* **2018**, *148*, 124117.
- (13) Dunlap, B. I. Robust and Variational Fitting. *Phys. Chem. Chem. Phys. PCCP* **2000**, *2*, 2113–2116.
- (14) Pierce, K.; Rishi, V.; Valeev, E. F. Robust Approximation of Tensor Networks: Application to Grid-Free Tensor Factorization of the Coulomb Interaction. *J. Chem. Theory Comput.* **2021**, *17*, 2217–2230.
- (15) Pierce, K.; Valeev, E. F. Efficient Construction of Canonical Polyadic Approximations of Tensor Networks. *J. Chem. Theory Comput.* **2023**, *19*, 71–81.
- (16) Pierce, K.; Morales, M. Using Matrix-Free Tensor-Network Optimizations to Construct a Reduced-Scaling and Robust Second-Order Møller-Plesset Theory. *ArXiv* **2025**,
- (17) Crawford, T. D.; Schaefer, H. F. Reviews in Computational Chemistry - Google Books. *Rev. Comput. Chem.* **2000**,
- (18) Čížek, J. On the Correlation Problem in Atomic and Molecular Systems. Calculation of Wavefunction Components in Ursell-Type Expansion Using Quantum-Field Theoretical Methods. *J. Chem. Phys.* **1966**, *45*, 4256–4266.

- (19) Cizek, J. *Adv. Chem. Phys.*; John Wiley and Sons, Inc.: Hoboken, NJ, USA, 2007; pp 35–89.
- (20) Cizek, J.; Paldus, J. Correlation problems in atomic and molecular systems III. Rederivation of the coupled-pair many-electron theory using the traditional quantum chemical methodst. *Int. J. Quantum Chem.* **1971**, *5*, 359–379.
- (21) Tajti, A.; Szalay, P. G.; Császár, A. G.; Kállay, M.; Gauss, J.; Valeev, E. F.; Flowers, B. A.; Vázquez, J.; Stanton, J. F. HEAT: High Accuracy Extrapolated Ab Initio Thermochemistry. *J. Chem. Phys.* **2004**, *121*, 11599–11613.
- (22) Harding, M. E.; Vázquez, J.; Ruscic, B.; Wilson, A. K.; Gauss, J.; Stanton, J. F. High-Accuracy Extrapolated Ab Initio Thermochemistry. III. Additional Improvements and Overview. *J. Chem. Phys.* **2008**, *128*, 114111.
- (23) Thorpe, J. H.; Lopez, C. A.; Nguyen, T. L.; Baraban, J. H.; Bross, D. H.; Ruscic, B.; Stanton, J. F. High-accuracy extrapolated ab initio thermochemistry. IV. A modified recipe for computational efficiency. *J. Chem. Phys.* **2019**, *150*, 224102.
- (24) Purvis, G. D.; Bartlett, R. J. A Full Coupled-Cluster Singles and Doubles Model: The Inclusion of Disconnected Triples. *J. Chem. Phys.* **1982**, *76*, 1910.
- (25) Beebe, N. H. F.; Linderberg, J. Simplifications in the Generation and Transformation of Two-Electron Integrals in Molecular Calculations. *Int. J. Quantum Chem.* **1977**, *12*, 683–705.
- (26) Löwdin, P.-O. Studies in Perturbation Theory. IX. Connection between Various Approaches in the Recent Development—Evaluation of Upper Bounds to Energy Eigenvalues in Schrödinger’s Perturbation Theory. *J. Math. Phys.* **1965**, *6*, 1341–1353.
- (27) Lowdin, P.-O. Some properties of inner projections. *Int. J. Quantum Chem.* **2009**, *5*, 231–237.

- (28) Folkestad, S. D.; Kjøenstad, E. F.; Koch, H. An efficient algorithm for Cholesky decomposition of electron repulsion integrals. *J. Chem. Phys.* **2019**, *150*, 194112.
- (29) Weigend, F.; Köhn, A.; Hättig, C. Efficient Use of the Correlation Consistent Basis Sets in Resolution of the Identity MP2 Calculations. *J. Chem. Phys.* **2002**, *116*, 3175.
- (30) Hättig, C. Optimization of auxiliary basis sets for RI-MP2 and RI-CC2 calculations: Core-valence and quintuple- ζ basis sets for H to Ar and QZVPP basis sets for Li to Kr. *Phys. Chem. Chem. Phys.* **2005**, *7*, 59–66.
- (31) DePrince, A. E.; Sherrill, C. D. Accuracy and Efficiency of Coupled-Cluster Theory Using Density Fitting/Cholesky Decomposition, Frozen Natural Orbitals, and a t_1 -Transformed Hamiltonian. *J. Chem. Theory Comput.* **2013**, *9*, 2687–2696.
- (32) Friesner, R. A. Solution of Self-Consistent Field Electronic Structure Equations by a Pseudospectral Method. *Chem. Phys. Lett.* **1985**, *116*, 39–43.
- (33) Friesner, R. A. Solution of the Hartree–Fock equations by a pseudospectral method: Application to diatomic molecules. *J. Chem. Phys.* **1986**, *85*, 1462–1468.
- (34) Langlois, J.; Muller, R. P.; Coley, T. R.; Goddard, W. A.; Ringnalda, M. N.; Won, Y.; Friesner, R. A. Pseudospectral generalized valence-bond calculations: Application to methylene, ethylene, and silylene. *J. Chem. Phys.* **1990**, *92*, 7488–7497.
- (35) Ringnalda, M. N.; Belhadj, M.; Friesner, R. A. Pseudospectral Hartree–Fock Theory: Applications and Algorithmic Improvements. *J. Chem. Phys.* **1990**, *93*, 3397–3407.
- (36) Friesner, R. A. New Methods For Electronic Structure Calculations on Large Molecules. *Annu. Rev. Phys. Chem.* **1991**, *42*, 341–367.
- (37) Martinez, T. J.; Carter, E. A. Pseudospectral multireference single and double excitation configuration interaction. *J. Chem. Phys.* **1995**, *102*, 7564–7572.

- (38) Martinez, T. J.; Mehta, A.; Carter, E. A. Pseudospectral Full Configuration Interaction. *J. Chem. Phys.* **1992**, *97*, 1876–1880.
- (39) Martinez, T. J.; Carter, E. A. Pseudospectral Møller–Plesset perturbation theory through third order. *J. Chem. Phys.* **1994**, *100*, 3631–3638.
- (40) Ko, C.; Malick, D. K.; Braden, D. A.; Friesner, R. A.; Martínez, T. J. Pseudospectral time-dependent density functional theory. *J. Chem. Phys.* **2008**, *128*, 104103.
- (41) Martinez, T. J.; Carter, E. A. Pseudospectral double excitation configuration interaction. *J. Chem. Phys.* **1993**, *98*, 7081–7085.
- (42) Hohenstein, E. G.; Parrish, R. M.; Martínez, T. J. Tensor Hypercontraction Density Fitting. I. Quartic Scaling Second- and Third-Order Møller–Plesset Perturbation Theory. *J. Chem. Phys.* **2012**, *137*, 044103.
- (43) Hohenstein, E. G.; Parrish, R. M.; Sherrill, C. D.; Martínez, T. J. Communication: Tensor Hypercontraction. III. Least-squares Tensor Hypercontraction for the Determination of Correlated Wavefunctions. *J. Chem. Phys.* **2012**, *137*, 221101.
- (44) Parrish, R. M.; Hohenstein, E. G.; Martínez, T. J.; Sherrill, C. D. Tensor Hypercontraction. II. Least-squares Renormalization. *J. Chem. Phys.* **2012**, *137*, 224106.
- (45) Hohenstein, E. G.; Kokkila, S. I. L.; Parrish, R. M.; Martinez, T. J. Quartic scaling second-order approximate coupled cluster singles and doubles via tensor hypercontraction: THC-CC2. *J. Chem. Phys.* **2013**, *138*, 124111.
- (46) Parrish, R. M.; Sherrill, C. D.; Hohenstein, E. G.; Kokkila, S. I. L.; Martínez, T. J. Communication: Acceleration of Coupled Cluster Singles and Doubles via Orbital-Weighted Least-Squares Tensor Hypercontraction. *J. Chem. Phys.* **2014**, *140*, 181102.
- (47) Shenvi, N.; Van Aggelen, H.; Yang, Y.; Yang, W.; Schwerdtfeger, C.; Mazziotti, D.

- Low rank factorization of the Coulomb integrals for periodic coupled cluster theory. *J. Chem. Phys.* **2013**, *139*, 54110.
- (48) Schutski, R.; Zhao, J.; Henderson, T. M.; Scuseria, G. E. Tensor-structured coupled cluster theory. *J. Chem. Phys.* **2017**, *147*, 184113.
- (49) Parrish, R. M.; Zhao, Y.; Hohenstein, E. G.; Martínez, T. J. Rank reduced coupled cluster theory. I. Ground state energies and wavefunctions. *J. Chem. Phys.* **2019**, *150*, 164118.
- (50) Lee, J.; Lin, L.; Head-Gordon, M. Systematically Improvable Tensor Hypercontraction: Interpolative Separable Density-Fitting for Molecules Applied to Exact Exchange, Second- and Third-Order Møller-Plesset Perturbation Theory. *J. Chem. Theory Comput.* **2020**, *16*, 243–263.
- (51) Hummel, F.; Tsatsoulis, T.; Grüneis, A. Low Rank Factorization of the Coulomb Integrals for Periodic Coupled Cluster Theory. *J. Chem. Phys.* **2017**, *146*, 124105.
- (52) Song, C.; Martínez, T. J. Analytical Gradients for Tensor Hyper-Contracted MP2 and SOS-MP2 on Graphical Processing Units. *J. Chem. Phys.* *147*, 161723.
- (53) Hohenstein, E. G.; Zhao, Y.; Parrish, R. M.; Martínez, T. J. Rank reduced coupled cluster theory. II. Equation-of-motion coupled-cluster singles and doubles. *J. Chem. Phys.* **2019**, *151*, 164121.
- (54) Hohenstein, E. G.; Martínez, T. J. GPU acceleration of rank-reduced coupled-cluster singles and doubles. *J. Chem. Phys.* **2021**, *155*, 184110.
- (55) Hohenstein, E. G.; Fales, B. S.; Parrish, R. M.; Martínez, T. J. Rank-reduced coupled-cluster. III. Tensor hypercontraction of the doubles amplitudes. *J. Chem. Phys.* **2022**, *156*, 054102.

- (56) Jiang, A.; Turney, J. M.; Schaefer, H. F. Tensor Hypercontraction Form of the Perturbative Triples Energy in Coupled-Cluster Theory. *Journal of Chemical Theory and Computation* **2022**, *19*, 1476–1486.
- (57) Zhao, T.; Simons, M.; Matthews, D. A. Open-Shell Tensor Hypercontraction. *Journal of Chemical Theory and Computation* **2023**, *19*, 3996–4010.
- (58) Datar, A.; Matthews, D. A. Robust Tensor Hypercontraction of the Particle–Particle Ladder Term in Equation-of-Motion Coupled Cluster Theory. *Journal of Chemical Theory and Computation* **2024**, *20*, 708–720.
- (59) Carroll, J. D.; Chang, J.-J. Analysis of Individual Differences in Multidimensional Scaling via an N-Way Generalization of “Eckart-Young” Decomposition. *Psychometrika* **1970**, *35*, 283–319.
- (60) Harshman, R. A. Foundations of the PARAFAC Procedure: Models and Conditions for an “Explanatory” Multimodal Factor Analysis. *UCLA Work. Pap. Phon.* **1970**, *16*, 1–84.
- (61) Hastad, J. Tensor rank is NP-complete. *Algorithms* **1990**, *11*, 644–654.
- (62) Hillar, C. J.; Lim, L.-H. Most Tensor Problems Are NP-Hard. *J. ACM* **2013**, *60*, 1–39.
- (63) Benedikt, U.; Auer, A. A.; Espig, M.; Hackbusch, W. Tensor Decomposition in Post-Hartree–Fock Methods. I. Two-electron Integrals and MP2. *J. Chem. Phys.* **2011**, *134*, 054118.
- (64) Benedikt, U.; Bohm, K.-H.; Auer, A. A. Tensor decomposition in post-Hartree–Fock methods. II. CCD implementation. *J. Chem. Phys.* **2013**, *139*, 224101.
- (65) Benedikt, U.; Auer, H.; Espig, M.; Hackbusch, W.; Auer, A. Tensor representation techniques in post-Hartree–Fock methods: matrix product state tensor format. *Mol. Phys.* **2013**, *111*, 2398–2413.

- (66) Böhm, K. H.; Auer, A. A.; Espig, M. Tensor representation techniques for full configuration interaction: A Fock space approach using the canonical product format. *J. Chem. Phys.* **2016**, *144*, 244102.
- (67) Kroonenberg, P. M.; de Leeuw, J. Principal Component Analysis of Three-Mode Data by Means of Alternating Least Squares Algorithms. *Psychometrika* **1980**, *45*, 69–97.
- (68) Beylkin, G.; Mohlenkamp, M. J. Numerical Operator Calculus in Higher Dimensions. *Proc. Natl. Acad. Sci.* **2002**, *99*, 10246–10251.
- (69) Calvin, J. A.; Peng, C.; Rishi, V.; Kumar, A.; Valeev, E. F. Many-Body Quantum Chemistry on Massively Parallel Computers. *Chem. Rev.* **2021**, *121*, 1203–1231.
- (70) Jørgensen, P.; Simons, J. Ab Initio Analytical Molecular Gradients and Hessians. *J. Chem. Phys.* **1983**, *79*, 334–357.
- (71) Wales, D. J.; Hodges, M. P. Global minima of water clusters (H₂O)_n, n ≤ 21, described by an empirical potential. *Chem. Phys. Lett.* **1998**, *286*, 65–72.
- (72) Peterson, K. A.; Adler, T. B.; Werner, H.-J. Systematically Convergent Basis Sets for Explicitly Correlated Wavefunctions: The Atoms H, He, B-Ne, and Al-Ar. *J. Chem. Phys.* **2008**, *128*, 084102.
- (73) Lesiuk, M. Implementation of the Coupled-Cluster Method with Single, Double, and Triple Excitations Using Tensor Decompositions. *J. Chem. Theory Comput.* **2020**, *16*, 453–467.